THE JOURNAL OF BIOLOGICAL CHEMISTRY
Vol. 275, No. 30, Issue of July 28, pp. 23082–23088, 2000

Printed in U.S.A.

Biochemical Evidence for the Involvement of Tyrosine in Epoxide Activation during the Catalytic Cycle of Epoxide Hydrolase*

Received for publication, February 22, 2000, and in revised form, May 3, 2000
Published, JBC Papers in Press, May 10, 2000, DOI 10.1074/jbc.M001464200

Takashi Yamada‡, Christophe Morisseau‡, Joseph E. Maxwell‡, Maria A. Argiriadi§¶, David W. Christianson§, and Bruce D. Hammock‡‖

From the ‡Department of Entomology, University of California, Davis, California 95616-8584 and §Roy and Diana Vagelos Laboratories, Department of Chemistry, University of Pennsylvania, Philadelphia, Pennsylvania 19104-6323

Epoxide hydrolases (EH) catalyze the hydrolysis of epoxides and arene oxides to their corresponding diols. The crystal structure of murine soluble EH suggests that Tyr^{465} and Tyr^{381} act as acid catalysts, activating the epoxide ring and facilitating the formation of a covalent intermediate between the epoxide and the enzyme. To explore the role of these two residues, mutant enzymes were produced and the mechanism of action was analyzed. Enzyme assays on a series of substrates confirm that both Tyr^{465} and Tyr^{381} are required for full catalytic activity. The kinetics of chalcone oxide hydrolysis show that mutation of Tyr^{465} and Tyr^{381} decreases the rate of binding and the formation of an intermediate, suggesting that both tyrosines polarize the epoxide moiety to facilitate ring opening. These two tyrosines are, however, not implicated in the hydrolysis of the covalent intermediate. Sequence comparisons showed that Tyr^{465} is conserved in microsomal EHs. The substitution of analogous Tyr^{374} with phenylalanine in the human microsomal EH dramatically decreases the rate of hydrolysis of *cis*-stilbene oxide. These results suggest that these tyrosines perform a significant mechanistic role in the substrate activation by EHs.

Epoxide hydrolases (EH,[1] EC3.3.2.3) hydrolyze epoxides and arene oxides to their corresponding diols (1). These enzymes are widely distributed among many species, including bacteria, fungi, plants, insects, and mammals (2–5). In mammals, there are two major classes of EH with broad and complementary substrate selectivity, soluble EH (sEH) and microsomal EH (mEH) (6). sEH participates not only in xenobiotic detoxification but also endogenous lipid metabolism, acting on epoxides of linoleic acid (leukotoxin and isoleukotoxin) (7) and arachidonic acid (*cis*-epoxyeicosatrienoic acids) (8). Elevated titers of linoleate and arachidonic acid diols are, respectively, thought to be associated with the inflammatory disorder known as acute respiratory distress syndrome (7) and pregnancy-induced hypertension (9). Inhibition of epoxide hydration may accordingly have a therapeutic value for these two serious disorders. Alternately, mEH appears to be mainly involved in the metabolism of xenobiotic epoxides (6). A protein-reactive and cytotoxic epoxide, naphthalene epoxide for example, is converted to the less toxic diol by this enzyme (10). The mEH is also related to activation of other arene oxides such as 7,12-dimethylbenzanthracene, a member of the polycyclic aromatic hydrocarbon class of chemical carcinogens (11). To understand xenobiotic toxicity, metabolic aberrations associated with pathological disorders, and to develop possible therapies against these, it is important to elucidate the molecular basis of EH catalysis.

The EHs belong to the α/β hydrolase fold family. These enzymes characteristically employ a two-step mechanism in which a catalytic nucleophile of the enzymes attacks a polarized electrophilic substrate, and the covalent intermediate is subsequently hydrolyzed (Fig. 1) (6). The mechanism of murine sEH has been mainly elucidated from a series of experiments utilizing heavy isotopes, protein mass spectrometry, and site-directed mutagenesis (12, 13). They indicated that Asp^{333} acts as a catalytic nucleophile and that a water molecule is activated by the nearby His^{523} and Asp^{495} pair (Fig. 1). This mechanism was extended to other EHs (2, 14–18). However, one or more additional amino acids are likely involved in the catalytic cycle especially in the activation of the epoxide ring (5), based on the mechanism of the haloalkane dehalogenase, HLD1, from *Xantobacter autotrophicus* G10, a related α/β hydrolase (6). Kinetics of the hydrolysis of chalcone oxide by sEH support this hypothesis. Thus a generalized scheme is postulated in which one or more amino acid(s) may polarize the epoxide oxygen by an acid-like mechanism, weakening the C-O epoxide bond and facilitating the attack on the carbon of the epoxide ring by a nucleophile, such as the conjugate base, Asp^{333} (19). Recently, the crystal structure of murine sEH has been determined at 2.8 Å resolution (20). The structure supports the previously proposed mechanism and suggests that Tyr^{465} and Tyr^{381} are the possible acid catalysts that activate the epoxide ring (Fig. 1). Additionally, analysis of the crystal structure of EH from *Agrobacterium radiobacter*, AD1, likewise suggested that Tyr^{152}-Tyr^{215} in this prokaryotic enzyme may have the same function (21). Thus, biochemical evidence is required to verify the mechanism of epoxide activation and to complement structure-based prediction.

In this study, site-directed mutagenesis was utilized to explore the role of Tyr^{465} and Tyr^{381} in the catalytic mechanism

* This work was supported in part by NIEHS, National Institutes of Health Grant R01-ES02710, NIEHS, National Institutes of Health Superfund Basic Research Program Grant ES04699, NIEHS, National Institutes of Health Center for Environmental Health Sciences Grant 1P30-ES05707, and National Institutes of Health Grant GM56838. The costs of publication of this article were defrayed in part by the payment of page charges. This article must therefore be hereby marked "*advertisement*" in accordance with 18 U.S.C. Section 1734 solely to indicate this fact.

¶ Current address: Laboratories of Molecular Biophysics, The Rockefeller University, 1230 York Ave., New York, NY 10021.

‖ To whom reprint requests should be addressed: Dept. of Entomology, One Shields Ave., University of California, Davis, CA 95616-8584. Tel.: 530-752-7519; Fax: 530-752-1537; E-mail: bdhammock@ucdavis.edu.

[1] The abbreviations used are: EH, epoxide hydrolase; sEH, soluble epoxide hydrolase; mEH, microsomal epoxide hydrolase; NEP2C, 4-nitrophenyl-2,3-epoxy-3-phenylpropyl carbonate; tDPPO, *trans*-1,3-diphenylpropene oxide; ESA, *cis*-9,10-epoxystearic acid; tSO, *trans*-stilbene oxide; cSO, *cis*-stilbene oxide; JH III, juvenile hormone III; FCO, 4-fluorochalcone oxide.

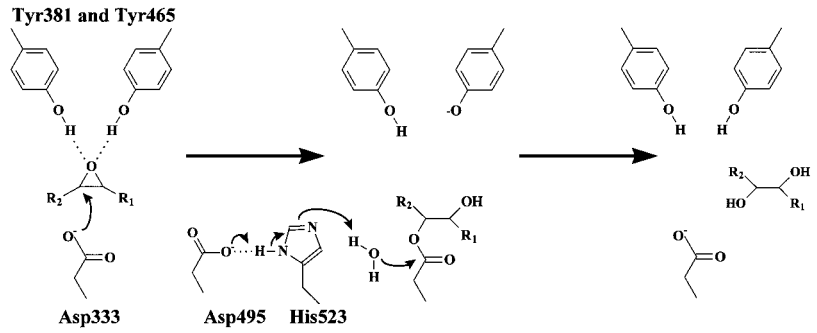

FIG. 1. **Two step mechanism of murine sEH.** In the first step, a reactive nucleophile Asp^{333} attacks the epoxide ring leading to the ring opening and the formation of hydroxyalkyl enzyme. In the second step, the covalent intermediate is hydrolyzed by a water molecule activated by a His^{523}-Asp^{495} pair. Tyr^{381} and Tyr^{465} are proposed to polarize the epoxide moiety to facilitate the attack by nucleophilic Asp^{333} (20, 26).

of murine sEH. The sEH variants were subjected to a series of enzyme assays and kinetic studies to assess their impact on epoxide activation. Additionally, this work was extended to Tyr^{374} of human mEH. Interpreted in view of the EH crystal structure, these results clearly support the role of active site tyrosine residues in epoxide activation by eukaryotic sEH and mEH.

EXPERIMENTAL PROCEDURES

Chemicals—The following compounds were previously synthesized in our laboratory: racemic 4-nitrophenyl-2,3-epoxy-3-phenylpropyl carbonate (NEP2C, compound **1**) (22); [^{3}H]*trans*-1,3-diphenylpropene oxide (tDPPO, compound **2**); [^{14}C]*cis*-9,10-epoxystearic acid (ESA, compound **4**) (23); [^{3}H]*trans*-stilbene oxide (tSO, compound **3**); [^{3}H]*cis*-stilbene oxide (cSO, compound **16**) (24); *para*-substituted chalcone oxides (compounds **6**-**11**) (19); compounds **13** and **15** (25); and compound **14** (26). [^{3}H]Juvenile hormone III (JH III; compound **5**) was obtained from NEN Life Science Products. Compound **12** was purchased from Aldrich.

Construction of Mutant Murine sEH—Sequence numbers are based on the murine sEH sequence (GenBank™/EMBL Data Bank accession number L05781) and human mEH sequence (X07936). Murine sEH cDNA or human mEH cDNA (27) was inserted into the *Eco*RI or *Bam*HI site of baculovirus expression vector, pFastBac1 (Life Technologies, Inc.). The whole plasmid was directly subjected to site-directed mutagenesis based on a *PfuTurbo* DNA polymerase system (Stratagene, La Jolla, CA). Oligonucleotides for murine sEH mutants were as follows: Y381F, 5′-CCAGTTTTCAATTTTCAGCTGTACTTT-3′ and 5′-AAAGTACAGCTGAAAATTGAAAACTGG-3′; Y465F, 5′-CCTCTGAACTGGTTCCGGAACACAGAA-3′ and 5′-GGAGACTTGACCAAGGCCTTGTGTCTT-3′; Y465A, 5′-CCTCTGAACTGGGGCCGGAACACAGAA-3′ and 5′-GGAGACTTGACCCCGGCCTTGTGTCTT-3′. Y381F/Y465F double mutant was constructed with the plasmid for Y465F and a set of oligonucleotides for Y381F. Oligonucleotides for human mEH mutant were as follows: Y374F, 5′-TCCCAGCGCTTCTTCAAGGAGAACCTG-3′ and 5′-CAGGTTCTCCTTGAAGAAGCGCTGGGA-3′. The mEH cDNA was obtained from Drs. C. Omiecinski and V. P. Hosagrahara (Seattle, WA). Underlined residues were modified to generate corresponding mutations. Effective mutations were verified by DNA sequencing of both strands.

Expression of Wild-type, Mutant Murine sEH, and Human mEH—Enzymes were produced using BAC-TO-BAC Baculovirus Expression System (Life Technologies, Inc.). Cells from *Trichoplusia ni* (*T. ni* High5) (500 ml, 5×10^5 cells/ml) were infected with virus solution at a multiplicity of infection of 0.1. Three days postinfection, the cells were resuspended in 20 ml of 0.1 M sodium phosphate buffer (pH 7.4) (buffer A) containing 1 mM phenylmethylsulfonyl fluoride, EDTA, and dithiothreitol, and homogenized with a Polytron. The crude extract was centrifuged at $12{,}000 \times g$ for 20 min. The supernatant was centrifuged again at $100{,}000 \times g$ for 1 h. For murine sEH, the resulting supernatant (cytosol fraction) was stored at −80 °C, and for human mEH, the pellet (microsomal fraction) was resuspended in 3 ml of buffer A and stored at −80 °C.

Protein Analysis—Protein concentrations were determined with the Pierce BCA assay (Pierce) using bovine serum albumin as a standard. SDS-polyacrylamide gel electrophoresis was performed according to Laemmli (28) using a 10% resolving gel. Assays for murine sEH, employing Western blot techniques, were performed using the corresponding polyclonal antibody as described previously (12). The polyclonal antibody for human mEH was a gift of Drs. Franz Oesch and Michael Arand (Mainz, Germany). Estimation of protein bands was carried out with the Scion Image software package (Scion, Frederick, MD).

Enzyme Assay—The sEH enzyme activity of the sEH wild type and its mutants was determined using five different substrates (compounds **1**-**5**). These assays were performed as described previously: NEP2C (**1**) (19), tDPPO (**2**) (23), tSO (**3**) (24), [^{14}C]ESA (**4**) (23), and JH III (**5**) (23, 29). The assays were run at 30 °C for 1–30 min depending on the substrate and the mutant used. To compare specific activities between wild-type and the mutant enzymes, identical concentrations of enzymes were used as judged by Western blot ([E] = 80 nM for **1, 3, 4, 5** and 3 nM for **2**). For the human microsomal EH, cSO (compound **16**) was used as substrate. Assay was performed as described (24) using 1 μg of the microsomal fraction. The wild-type enzyme was incubated at 30 °C for 1 min, while the Y374F mutant was incubated for 30 min. Cytosol fractions of control cells have no detectable epoxide hydrolase activities above background (30).

Kinetic Assay Conditions—The kinetic constants were determined using the two-step inhibition model previously described for EH inhibition, where chalcone oxides and NEP2C were used as substrate (19). Inhibitor concentrations between 0 and 2.5 μM were used for the wild-type enzyme, whereas concentrations between 0 and 50 μM were used for the two mutant enzymes. To achieve homogeneity in the results and to be able to compare them between the wild-type and the two mutants, Y381F and Y465F, identical concentrations of enzymes (80 nM) were used as determined by Western blot. Measurements were made in the presence of excess of substrate ([S] = 40 μM). Activity measurements at 0–30 s post inhibitor introduction allow determination of the initial rate of enzyme inhibitor complex formation (ρ) as described previously (19). Under these conditions, less than 10% of the inhibitor was bound to the enzyme. The enzyme-inhibitor dissociation constant (K_d) and the rate of enzyme-inhibitor covalent complex formation (k_2) were calculated from plots of ρ *versus* [*I*] (19). The rates of dealkylation and product release (k_3) were calculated from enzyme activities in 1:1 enzyme:inhibitor mixtures, at times varying between 1 and 20 min post inhibitor introduction as described previously (19). The decomposition rate of the inhibitors in the absence of the enzyme was found to be negligible (<1%) over the period studied. The accuracy of the applied kinetic model was assessed by comparing theoretical and measured results for ρ, producing correlation factors greater than 0.95. Based on experimental inhibitor and substrate concentrations, a maximal error in observed K_d of ~5% can be attributed to incomplete dissociation of *EI*. Moreover, the k_2 and k_3 values obtained indicated a 7% maximal error in k_2 because of the *EC* degradation.

IC_{50} Assay—IC_{50} values were determined using tDPPO (compound **2**) as a substrate. Enzymes (3 nM) were incubated with inhibitors for 5 min at 30 °C prior to substrate introduction ([S] = 50 μM). Assays were run for 1 min for wild-type and were extended to 15 min for Y381F and Y465F. IC_{50} was calculated by linear regression of five datum points with a minimum of two points of either side of IC_{50}. The results were generated from at least three separate runs each in triplicate to obtain the standard deviation.

Graphic Analysis—Images used in this study were rendered and displayed in the Swiss-Pdb Viewer (31–33) using coordinates supplied by Argiriadi *et al.* (26). Additional graphic enhancements were performed in the Photoshop graphic programming environment.

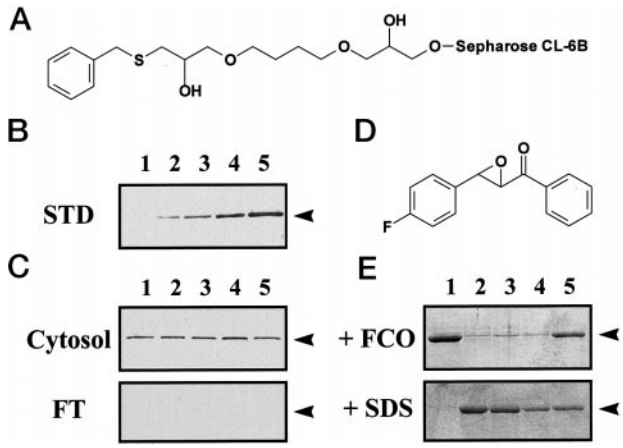

FIG. 2. **Western blot and purification of wild-type and mutant murine sEH.** *A,* structure of affinity ligand for purification of murine sEH. *B,* Western blot of purified murine sEH for protein standard (*STD*). *Lane 1,* 0 ng; *lane 2,* 100 ng; *lane 3,* 200 ng; *lane 4,* 300 ng; *lane 5,* 400 ng. *C,* Western blot of wild-type and mutant murine sEH for cytosol and flow through (*FT*) fractions. Cytosol fraction prepared from baculovirus infected *T. ni* High5 cells was applied to affinity column, and the flow through fraction was recovered. SDS-polyacrylamide gel electrophoresis was performed to quantify the sEH so a similar quantity of sEH protein could be used for kinetic studies. *Lane 1,* wild-type (2.5 μg); *lane 2,* Y381F (1.3 μg); *lane 3,* Y465F (2.5 μg); *lane 4,* Y465A (4.5 μg); *lane 5,* Y381F/Y465F (0.63 μg). *D,* structure of the eluting agent FCO. *E,* elution of wild-type and mutant murine sEH. In the first step, 1 mM FCO in buffer A was applied to affinity column. In the second step, 1% SDS was applied to the column. Equivalent volumes of the fractions were loaded onto SDS-polyacrylamide gel electrophoresis for each enzyme. *Lane 1,* wild-type; *lane 2,* Y381F; *lane 3,* Y465F; *lane 4,* Y465A; *lane 5,* Y381F/Y465F.

RESULTS

Expression and Activities of Tyrosine Mutants of Murine sEH—To explore the role of each of the tyrosines of murine sEH, we prepared four different mutant constructs, Y381F, Y465F, Y465A, and Y381F/Y465F. The enzymes were subsequently produced using baculovirus expression system as described under "Experimental Procedures." In the purification of murine sEH, the ligand (Fig. 2*A*) interacts with the putative hydrophobic pocket near the active site (12, 34). Wild-type and mutant protein were detected at similar expression level in the cytosol fraction and not detected in the flow through fraction (Fig. 2*C*) indicating that the mutant enzyme probably maintained its structural integrity. The mutant enzymes were eluted in low yield with 1 mM 4-fluorochalcone oxide (FCO), a selective inhibitor for sEH, indicating probable lower affinity for the inhibitor (Fig. 2, *D–E*). Total protein eluted by FCO followed by SDS (Fig. 2*E*) was similar for both wild and mutant enzymes, indicating same overall binding for each.

The specific activities of the wild-type and mutant enzymes in the hydrolysis of five substrates are summarized in Table I. These substrates are classified, and ordered from the more reactive (NEP2C (compound **1**)) to the less reactive (JH III (compound **5**)). The specific activities of wild-type enzyme were similar to previously published results (19, 23). NEP2C and JH III are known to be hydrolyzed by esterases; however, the esterase-dependent hydrolysis was not detectable in these experiments (data not shown). In mutant enzymes, the activities were lower than those of the wild-type. Substrates containing less reactive epoxides resulted in larger changes in activity between the wild-type and the mutant enzymes, suggesting that hydrolysis of less reactive epoxides is dependent on activation by tyrosine(s). The Y381F/Y465F mutant demonstrated no detectable catalytic activity with any of the substrates used. These results suggest that both Tyr^{381} and Tyr^{465} are required for full activity of the murine sEH. This is consistent with the results of analogous experiments with bacterial EH showing that active site tyrosines Tyr^{152} and Tyr^{215} are important for catalysis (35).

Kinetics of Inhibition—To further investigate the role of the two residues Tyr^{381} and Tyr^{465} in the catalytic mechanism, we determined the kinetic constants of their inhibition by chalcone oxides. Chalcone oxides are in fact poor EH substrates that inhibit the enzyme by forming a stable covalent intermediate (19). Their action is described by the following equation.

$$E + I \underset{}{\overset{K_d}{\rightleftharpoons}} EI \overset{k_2}{\longrightarrow} EC \overset{k_3}{\longrightarrow} E + P \qquad \text{(Eq. 1)}$$

The nonlinear regression of the initial rate of *EC* formation (ρ) *versus* inhibitor concentration ([*I*]) permits the calculation of K_d and k_2 (19). The slope of the *EC* complex decomposition, $\ln(A_0 - A)$ *versus* time, permits the calculation of k_3 (19). Derived kinetic constants are listed in Table II.

Both mutations of Tyr^{465} and of Tyr^{381} by phenylalanine resulted in increases in the K_d values up to 50-fold, with the exception of compound **7** and the Tyr^{381} mutant (Table II). These results demonstrate that both tyrosines are implicated in the binding of the substrate. The change in K_d is well correlated ($r^2 = 0.91$) with the σ values of the *para*-substitution of chalcone oxides for Y465F, whereas no relationships were found for Y381F. The observed increased K_d in mutant enzymes reflect the smaller interaction between the enzyme and the inhibitor. The linear relation observed between K_d and σ for Y465F highlights the possible bond between Tyr^{465} and epoxide moiety, as stated (26).

The rate of alkylation (k_2) is also greatly altered in both mutations (Table II). The values of k_2 for Y465F decreased increasingly from 2- to 30-fold for compounds **11** to **6,** respectively. For Y381F such trends in the decreased k_2 were observed only from compound **9** to **6,** whereas compounds **11** to **9** showed a 7-fold decrease in their k_2 values. The Hammett plot (Fig. 3) showing the logarithm of the relative rates ($^{4-R}k_2/^{4-H}k_2$) *versus* the constant $\sigma+$ for each 4-position substituent illustrates this influence. These results were correlated with $\sigma+$ for the three enzymes, indicating that development of a relative positive charge at the reactive center is important for the alkylation step. For the wild-type enzyme, a linear relationship ($r^2 = 0.93$) with a slope of -0.56 was obtained, indicating a push-pull mechanism, in which the epoxide oxygen is activated by protonation facilitating a nucleophilic attack on the carbon of the epoxide ring by the Asp^{333} carboxylate anion (19). A linear relationship ($r^2 = 0.91$) was obtained for Y465F, indicating a consistent mechanism operating throughout the chalcone oxide series. However, the sign of the slope (+ 0.27) is inverted from the slope of the of the wild-type enzyme, indicating a different mechanism. This value is very close to the value (+0.32) found for a general basic mechanism of opening of similar epoxides (36). This result strongly suggests that a simple nucleophilic mechanism is implied in the action of Y465F and that Tyr^{465} is directly related to the polarization of the epoxide moiety. A bell shaped relationship was obtained for Y381F, indicating a change of mechanism operating throughout the chalcone oxide series. A slope (+0.26) similar to one of Y465F is obtained for the electron donating *para*-substitutions (**6** to **9**), whereas a slope (−0.51) similar to the one for wild type is obtained for electron withdrawing *para*-substitutions (**9** to **11**). Therefore, Tyr^{381} participates in the polarization of the epoxide moiety. However, its role is less clear than that of Tyr^{465}.

The rate of dealkylation k_3 was less influence by either of the tyrosine mutations; the decreased k_3 between 1- and 3-fold are observed for Y465F and Y381F compared with the wild type

TABLE I

Specific activities of wild-type and mutant murine sEH

All assays were performed on the cytosol fraction from baculovirus-infected *T. ni* cells. The reported results are the mean ± S.D. (n = 3). Levels of sEH protein were apparently identical in all assays based on Western blot.

Substrate	No.	Specific activity [nmol/min/mg protein]				
		Wild-type	Y381F	Y465F	Y465A	Y381F-Y465F
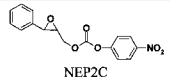 NEP2C	**1**	7370 ± 300	2830 ± 300	3820 ± 300	630 ± 70	n.d.[a]
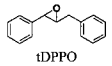 tDPPO	**2**	21800 ± 600	840 ± 60	770 ± 70	92 ± 7	n.d.
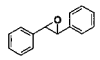 tSO	**3**	1810 ± 50	25 ± 2	12 ± 1	1.3 ± 0.2	n.d.
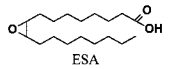 ESA	**4**	1520 ± 100	90 ± 4	27 ± 2	200 ± 10	n.d.
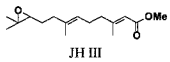 JH III	**5**	970 ± 30	30 ± 1	35 ± 1	10 ± 0.2	n.d.

[a] *n.d.*, nondetectable.

TABLE II

Kinetic constants for inhibition of wild-type and mutant murine sEH by chalcone oxides

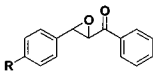

R:	No.	K_d (μM)[a]			k_2 (10^{-2} s^{-1})[a]			k_3 (10^{-4} s^{-1})[b]		
		Wild-type	Y465F	Y381F	Wild-type	Y465F	Y381F	Wild-type	Y465F	Y381F
CH_3O	**6**	2.4 ± 0.5	8 ± 2	8.8 ± 0.7	61 ± 9	1.9 ± 0.2	1.9 ± 0.1	40 ± 8	37 ± 6	23 ± 3
C_6H_5	**7**	0.33 ± 0.09	1.5 ± 0.4	0.36 ± 0.09	39 ± 6	2.8 ± 0.7	2.2 ± 0.1	10 ± 1	6.9 ± 0.9	16 ± 1
F	**8**	1.2 ± 0.3	30 ± 5	13 ± 3	37 ± 5	3.7 ± 0.3	2.9 ± 0.2	76 ± 23	22 ± 7	35 ± 11
H	**9**	2.0 ± 0.6	25 ± 5	20 ± 5	24 ± 4	4.0 ± 0.7	3.3 ± 0. 4	63 ± 2	28 ± 3	44 ± 6
Br	**10**	0.35 ± 0.07	8 ± 1	17 ± 5	18 ± 2	4.1 ± 0.3	2.5 ± 0.3	11 ± 1	7 ± 2	12 ± 1
NO_2	**11**	0.6 ± 0.1	32 ± 9	3.5 ± 0.9	9 ± 1	5.4 ± 0.7	1.3 ± 0.1	69 ± 14	28 ± 7	25 ± 6

[a] Value ± 95% confidence interval.
[b] Mean ± S.D. (n = 3).

(Table II). Moreover, no relation was found between the intensity of the change in k_3 and the nature of the *para*-substitution for Y465F and Y381F. These results indicate that neither tyrosine directly influences the hydrolysis of the enzyme-inhibitor covalent intermediate. This agrees with prediction from the crystal structure (20). Additionally, changes in specific activities for compounds **1**-**5** probably came from the changes in K_d and k_2, because k_3 was unchanged for compounds **6**-**11**.

Inhibition of Tyrosine Mutants by Ureas and Carbamate—The crystal structure of sEH-*N*-cyclohexyl-*N*′-decyl urea (compound **14**) complex shows that Tyr^{465} and Tyr^{381} provide hydrogen bond interaction with the carbonyl group of the urea (26). To evaluate this apparent binding trend with the tyrosines, IC_{50} values were determined for wild type and for both tyrosine mutants (Table III). Substitution of Tyr^{381} by phenylalanine resulted in an enzyme with 8–88-fold higher IC_{50} values for compounds tested. Replacement of Tyr^{465} by phenylalanine increased IC_{50} by 2–13-fold. These results suggest that both Tyr^{381} and Tyr^{465} interact with these inhibitors. Particularly Tyr^{381} seems more important than Tyr^{465} for binding with compounds **13** and **14**. Tyr^{465} may contribute less to the free energy of binding for these inhibitors than Tyr^{381}.

Mutagenesis of Tyr^{374} in Human mEH—Although human mEH has 21% sequence identity with murine sEH (5), the catalytic triad (Asp^{226}, Glu^{404}, and His^{431}) is conserved when compared with sEH (6). Sequence alignment shows that Tyr^{374} in human mEH seems to be analogous to Tyr^{465} in murine sEH (2). The tyrosine is conserved in all sequenced mEHs (20, 21). As shown in Fig. 4*A*, the linear distance between these amino acids is similar in the primary structures of murine sEH and human mEH. Tyr^{283} or Tyr^{291} in human mEH could correspond to Tyr^{381} in murine sEH. However, the tyrosines are not conserved in all mEHs (20, 21). Thus only the Tyr^{374} mutant was made to explore the role of the residue in this enzyme. As shown in Fig. 4*B*, wild-type and Y374F enzymes were expressed in the microsomal fraction at similar levels. Specific activity was determined for the hydrolysis of *cis*-stilbene oxide (compound **16**), which is selective for mEH. Compared with wild-type enzyme, the Y374F mutant had dramatically decreased activity (Fig. 4*D*). The recent crystal structure of EH from *Aspergillus niger*, a soluble member of mEH, showed that Tyr^{314} likely plays a significant role in epoxide activation (37). The authors suggested that Tyr^{314} appears to be equivalent to Tyr^{374} in human mEH based on the sequence comparison between these two enzymes. Taken together, mutation of Tyr^{374} likely affects polarization of epoxide moiety rather than some other step in the catalytic cycle. This result suggests that involvement of tyrosine in the catalytic mechanism is common in both sEH and mEH.

DISCUSSION

In the present study, we examined the role of the tyrosines in the catalytic mechanism of EH. It had been proposed that the epoxide oxygen might be activated by a possible acid catalyst to

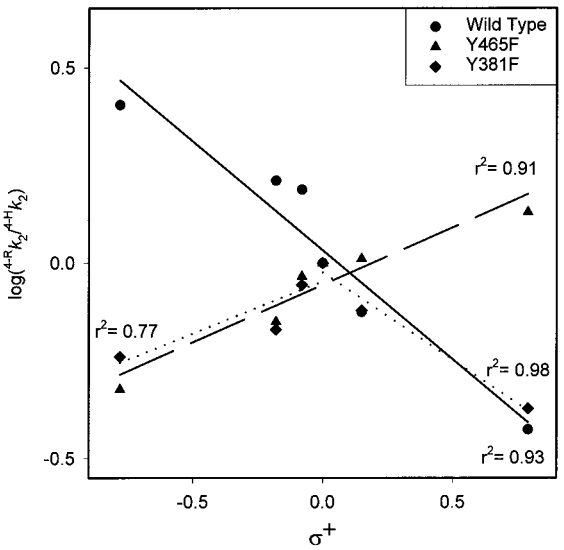

FIG. 3. **Log of the sEH-inhibitor complex relative rate of formation ($^{4\text{-R}}k_2/^{4\text{-H}}k_2$) for *para*-substituted chalcone oxides *versus* σ^+, the positive Hammett constant.** The log ratio of k_2 values for each *para*-substituted chalcone oxide to the unsubstituted chalcone oxide (compound **9**) from Table II were plotted *versus* electronic parameter σ^+. The slope of the lines indicates the type of mechanism involved and its intensity.

weaken the C-O bond of the epoxide ring and facilitate the attack by a nucleophilic aspartate (6). However, a variety of early studies showed that the reaction intermediate lacked full carbocation character (reviewed in Ref. 6). Based on the crystal structure of murine sEH (20, 26), we tested the hypothesis that Tyr^{465} and Tyr^{381} are involved in epoxide activation by examining the mutant enzymes.

The substitution of tyrosine with phenylalanine is not expected to create a significant conformational change, even locally, because the body of the tyrosine and phenylalanine are both partially buried and unchanged, whereas the changed region, the phenolic hydroxyl group, is in the solvent accessible region of the active site. We tested the hypothesis by showing that all mutant enzymes bind to the active site-directed affinity column with similar efficiency. This would not be expected if mutation caused a major alteration in the conformation of the enzyme. Our results are consistent with the prediction. The sEH variants bound on the affinity column were eluted by 1 mM FCO with lower recovery than the wild type. Because the affinity ligand is thought to interact with the putative hydrophobic tunnel close to the active site (34), the lower recovery in sEH variants might result from weaker competition with FCO (Fig. 2*E*). The larger K_d found for Y465F and Y381F in compound **8** (Table II) supports the possibility. Based on the results in Table II, one could expect compound **7** to give better elution; however, the decreased solubility overcame increased affinity for the enzymes. Such an effect also was observed for the wild-type enzyme (34). Y381F/Y465F was eluted by 1 mM FCO with relatively higher yield than other mutants. In this case, the loss of two hydroxyl groups may be contributing to a weaker interaction between the enzyme and affinity ligand. No change was seen in the mobility of the wild-type and mutant enzymes on isoelectric focusing (data not shown). Taken together these data suggest that the mutations do not cause dramatic conformational changes in the active site. We hypothesize that the decreased specific activities in the mutants (Table I) result largely from a loss of the hydroxyl group(s) in the active site.

The kinetics of hydrolysis of chalcone oxides suggests both Tyr^{465} and Tyr^{381} are implicated in the binding of substrate and in the formation of a hydroxyalkyl intermediate. Particularly, Tyr^{465} showed a linear relationship in decreased K_d and k_2 with *para*-substitution of chalcone oxides, indicating the amino acid directly polarizing epoxide moiety. In the complex of sEH and the potent urea inhibitor, *N*-cyclohexyl-*N*′-decyl urea, the carbonyl oxygen accepts the hydrogen bond from Tyr^{465} and Tyr^{381}, and one of the NH groups accepts the hydrogen bond from Asp^{333}. The side chain Gln^{382} additionally participates in a hydrogen bond interaction with the carbonyl oxygen of the urea (Fig. 5*A*). The binding nature suggests that the inhibitor mimics the transition state for epoxide ring opening in sEH catalysis (26). Our results are consistent with this structure-based prediction. Both mutations of the two tyrosines increased IC_{50} values for ureas tested (Table III). Because the epoxide substrates are susceptible to an S_N2 backside attack on the carbon of epoxide ring by nucleophilic Asp^{333} (13), the angle and distance of these two tyrosines are suitable to activate epoxide oxygen in concert with nucleophilic attack by Asp^{333}. Analysis of small molecule crystal structures contained in the Cambridge Structural Data base (38) yields 15 independent examples of hydrogen bonds donated from hydroxyl groups to epoxide oxygens with an average O-O separation of 2.8 Å. The scatter plot in Fig. 5*B* reveals that the hydrogen bond stereochemistry between the phenolic hydroxyl groups of Tyr^{465},

TABLE III
Inhibition of wild-type and mutant murine sEH by ureas and carbamate

IC_{50} values were determined using tDPPO (compound **2**) as a substrate. The reported results are the IC_{50} mean ± S.D. (n = 3).

Inhibitor	No.	IC_{50} (nM) Relative inhibition of wild type [fold]		
		Wild-type	Y381F	Y465F
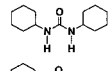	**12**	22 ± 1 [1]	169 ± 10 [8]	275 ± 10 [13]
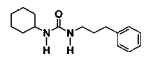	**13**	11 ± 1 [1]	131 ± 10 [12]	25 ± 3 [2]
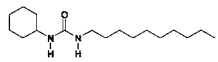	**14**	24 ± 4 [1]	2100 ± 130 [88]	48 ± 10 [2]
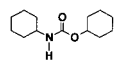	**15**	42 ± 2 [1]	891 ± 90 [21]	398 ± 20 [10]

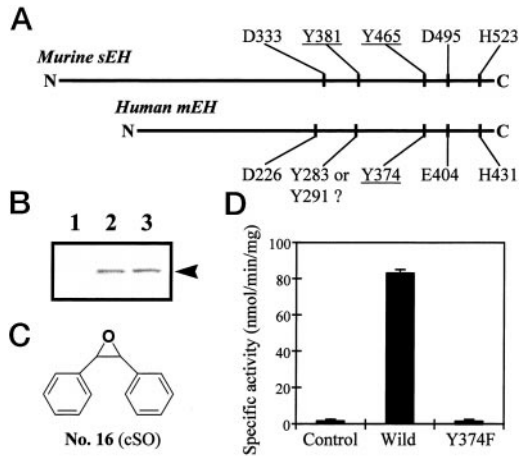

FIG. 4. **Mutagenesis of human mEH.** *A,* comparison of the catalytically important amino acids between murine sEH and human mEH. *Underlined* residues were modified to generate the mutant enzymes in this study. *B,* Western blot of wild-type and mutant human mEH in *T. ni* High5 cells using mEH polyclonal antibody. 10 μg of the microsomal protein was loaded onto SDS-polyacrylamide gel electrophoresis. *Lane 1,* control; *lane 2,* wild-type; *lane 3,* Y374F. Control represents the protein from the cells expressng LacZ. *C,* structure of cSO. *D,* specific activity of wild-type and mutant human mEH for cSO.

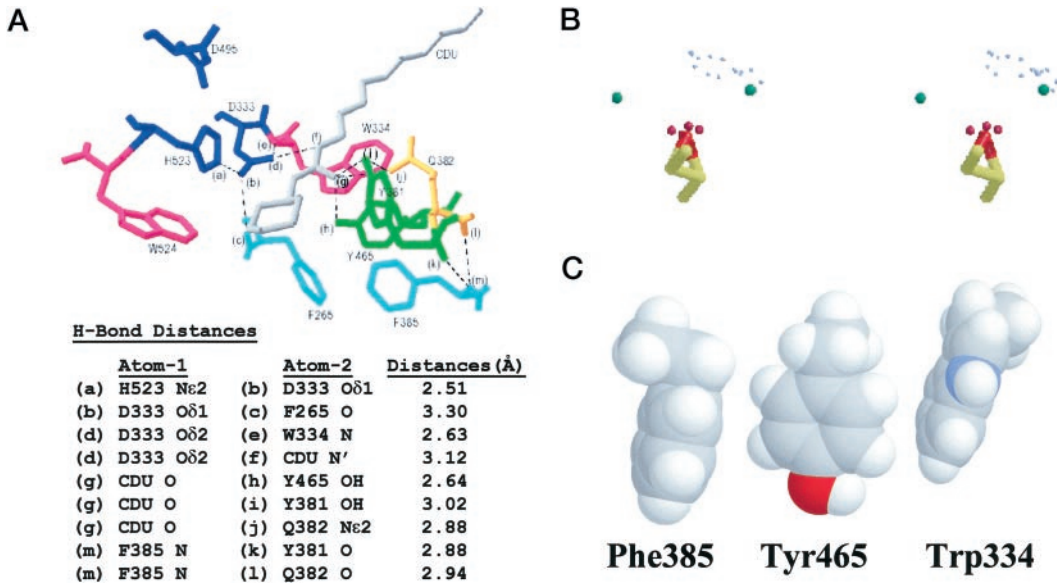

H-Bond Distances

Atom-1	Atom-2	Distances (Å)
(a) H523 Nε2	(b) D333 Oδ1	2.51
(b) D333 Oδ1	(c) F265 O	3.30
(d) D333 Oδ2	(e) W334 N	2.63
(d) D333 Oδ2	(f) CDU N′	3.12
(g) CDU O	(h) Y465 OH	2.64
(g) CDU O	(i) Y381 OH	3.02
(g) CDU O	(j) Q382 Nε2	2.88
(m) F385 N	(k) Y381 O	2.88
(m) F385 N	(l) Q382 O	2.94

FIG. 5. **Significant residues in the active site of murine sEH.** *A,* residues, considered as comprising "the catalytic triad" are presented in *blue*, tyrosines in *green*, tryptophans in *magenta,* and phenylalanines in *cyan*. Glu[382], suspected of involvement in possible conformational changes associated with binding is shown in *dark orange*. The potent urea inhibitor, *N*-cyclohexyl-*N′*-decyl urea (compound **14**) is shown in *gray* with the *N*,*N′* and O atoms of the urea moiety labeled. *B,* stereo view of a scatterplot of 15 hydrogen bond interactions between epoxide oxygen atoms and hydroxyl groups retrieved from the Cambridge Structural Data base (38). The epoxide group of each pair is superimposed onto the reference epoxide shown while allowing the hydroxyl oxygen position to "ride" into place (*light blue spheres*). The hydroxyl oxygens of Tyr[465] and Tyr[381] in a model of the sEH-substrate complex are also superimposed (*green spheres*) and are well within the expected range of optimal hydrogen bond stereochemistry reflected by the examples from the data base. *C,* amino acid polarizing the substrate. Tyr[465] is flanked by edge-to-face interactions with Phe[385] and Trp[334] that would stabilize the intermediate phenolate anion (20).

Tyr[381], and the substrate epoxide oxygen modeled into the sEH active site (26) is quite consistent with the preferred stereochemistry of such interactions reflected by the examples from the Cambridge Structural Data base. Epoxide-phenol hydrogen bond stereochemistry is also consistent with the preferred stereochemistry of hydrogen bonds to tyrosines in refined protein structures as outlined by Ippolito *et al.* (39). In the crystal structure of murine sEH, Tyr[465] is flanked by edge to face interactions with Trp[334] and Phe[385] (Fig. 5*C*). The interaction is thought to stabilize phenolate anion in the transition state (20). Similar interaction is found in the recent crystal structures of bacterial EH and fungus EH (21, 37). Our biochemical results highlight the significance of Tyr[465] in the epoxide activation.

Our preliminary results suggest that Tyr[374] in human mEH is analogous to Tyr[465] in murine sEH. The tyrosine is absolutely conserved in all EHs sequenced (20, 21). Although it is not known if Tyr[374] forms edge to face interaction with other aromatic amino acids, sequence alignment shows that Trp[227] and Phe[290] in human mEH likely correspond to Trp[334] and Phe[385] in murine sEH. Additional experiments will be required to address the question if a corresponding second tyrosine exists for mEH. Tyr[283] and Tyr[291] in human mEH may be equivalent to Tyr[381] in murine sEH on the basis of distance comparison (Fig. 4*A*). However, both tyrosines are not conserved in all mEHs (20, 21). Tyr[299] was suggested to be a possible second tyrosine in human mEH, based on the sequence comparison with fungus sEH. This fungus sEH belongs to the same class as mammalian mEH, although the sequence relationships were weak (37). There is another possibility that mEH may have only one tyrosine for activation. Genetic relationships suggest that mEH and sEH likely have diverged from common ancestor (5). Both enzymes are distantly related and have the same major amino acid side chain involved in hydrating epoxides. However, they are separated by a vast evolutionary distance (5) and have different substrate preference; sEH has an activity on less reactive epoxides such as arachidonic acid epoxides, and mEH on reactive epoxides such as arene oxides. The sEH is more active on epoxide substrates on linear system as one would anticipate from its active site being a tunnel rather than a groove (20).

EHs are members of the α/β hydrolase fold family-like esterases and haloalkane dehalogenases (5, 40). EHs and esterases have a common mechanism in hydrating substrates but a different nucleophile, aspartate and serine, respectively. The D333S mutant of murine sEH has no activity on epoxides (12). It was hypothesized that the mutant enzyme might acquire esterase activity with serine as a nucleophile. However, it had no hydrolytic activity on several esters.[2] The ester will be trigonal moving to tetrahedral as a transition state and transient intermediate interacting with NH moiety of two glycines and one alanine (41, 42). In contrast, the epoxide will be tetrahedral in the transition state interacting with OH moiety of two tyrosines. The absence of esterase activity in D333S can be explained in part by having an incorrect angle of the activating groups. Genetic relationships reveal that haloalkane dehalogenase and the sEH C-terminal catalytic domain are more related and might have been diverged from common ancestor (5). Both enzymes have a common nucleophilic aspartate (6). In haloalkane dehalogenase HLD1, however, two tryptophans (Trp[125] and Trp[175]) are responsible for the activation of the halide-leaving group (43). As shown in Fig. 5*A*, Trp[334] and Trp[524] conserved in the EH family are located near the active site in murine sEH. In the past, these two residues were proposed to activate the epoxide ring (14, 15). However, the orientation, angle, and distance are not suitable to activate the substrate epoxide, supporting the previous mutagenesis results of these tryptophans (14, 15). In addition, an epoxide likely needs more activation than a halide group does. These data suggest the possibility that EHs have acquired a unique mechanism for substrate activation through evolution. Alternately, lysine was

[2] B. D. Hammock, unpublished data.

previously postulated to be a proton-donating group (2, 5, 44). This residue is, however, not present in the active site (Fig. 5*A*).

In conclusion, we demonstrated the involvement of tyrosine in the activation of epoxide in the catalytic cycle of EH. The activation mechanism is apparently conserved within EH family and is likely unique in the α/β hydrolase fold family.

Acknowledgments—We thank Drs. C. Omiecinski and V. P. Hosagrahara (University of Washington, Seattle, WA) for the gift of the cDNA for human mEH. We gratefully acknowledge the technical advice of Dr. M. Derbel (University of California, Davis, CA) for baculovirus expression. We thank Drs. F. Oesch and M. Arand (University of Mainz, Mainz, Germany) for generously providing polyclonal antibody against human mEH.

REFERENCES

1. Oesch, F. (1973) *Xenobiotica* **3,** 305–340
2. Rink, R., Fennema, M., Smids, M., Dehmel, U., and Janssen, D. (1997) *J. Biol. Chem.* **272,** 14650–14657
3. Arand, M., Hemmer, H., Durk, H., Baratti, J., Archelas, A., Furstoss, R., and Oesch, F. (1999) *Biochem. J.* **344,** 273–280
4. Debernard, S., Morisseau, C., Severson, T. F., Feng, L., Wojtasek, H., Prestwich, G. D., and Hammock, B. D. (1998) *Insect Biochem. Mol. Biol.* **28,** 409–419
5. Beetham, J. K., Grant, D., Arand, M., Garbarino, J., Kiyosue, T., Pinot, F., Oesch, F., Belknap, W. R., Shinozaki, K., and Hammock, B. D. (1995) *DNA Cell Biol.* **14,** 61–71
6. Hammock, B., Grant, D., and Storms, D. (1997) in *Comprehensive Toxicology* (Sipes, I., McQueen, C., and Gandolfi, A., eds) Vol. 3, pp. 283–305, Pergamon, Oxford
7. Moghaddam, M. F., Grant, D. F., Cheek, J. M., Greene, J. F., Williamson, K. C., and Hammmock, B. D. (1997) *Nat. Med.* **3,** 562–566
8. Zeldin, D. C., Wei, S., Falck, J. R., Hammock, B. D., Snapper, J. R., and Capdevila, J. H. (1995) *Arch. Biochem. Biophys.* **316,** 443–451
9. Oltman, C., Weintraub, N., VanRollins, M., and Dellsperger, K. (1998) *Circ. Res.* **83,** 932–939
10. Tingle, M., Pirmohamed, M., Templeton, E., Wilson, A., Madden, S., Kitteringham, N., and Park, B. (1993) *Biochem. Pharmacol.* **46,** 1529–1538
11. Phillips, D., and Grover, P. (1994) *Drug. Metab. Rev.* **26,** 443–467
12. Pinot, F., Grant, D. F., Beetham, J. K., Parker, A. G., Borhan, B., Landt, S., Jones, A. D., and Hammock, B. D. (1995) *J. Biol. Chem.* **270,** 7968–7974
13. Borhan, B., Jones, A. D., Pinot, F., Grant, D. F., Kurth, M. J., and Hammock, B. D. (1995) *J. Biol. Chem.* **270,** 26923–26930
14. Arand, M., Wagner, H., and Oesch, F. (1996) *J. Biol. Chem.* **271,** 4223–4229
15. Laughlin, L. T., Tzeng, H. F., Lin, S., and Armstrong, R. N. (1998) *Biochemistry* **37,** 2897–2904
16. Tzeng, H. F., Laughlin, L. T., and Armstrong, R. N. (1998) *Biochemistry* **37,** 2905–2911
17. Arand, M., Muller, F., Mecky, A., Hinz, W., Urban, P., Pompon, D., Kellner, R., and Oesch, F. (1999) *Biochem. J.* **337,** 37–43
18. Lacourciere, G. M., and Armstrong, R. N. (1993) *J. Am. Chem. Soc.* **115,** 10466–10467
19. Morisseau, C., Du, G., Newman, J. W., and Hammock, B. D. (1998) *Arch. Biochem. Biophys.* **356,** 214–228
20. Argiriadi, M., Morisseau, C., Hammock, B., and Christianson, D. (1999) *Proc. Natl. Acad. Sci. U. S. A.* **96,** 10637–10642
21. Nardini, M., Ridder, I. S., Rozeboom, H. J., Kalk, K. H., Rink, R., Janssen, D. B., and Dijkstra, B. W. (1999) *J. Biol. Chem.* **274,** 14579–14586
22. Dietze, E. C., Kuwano, E., and Hammock, B. D. (1994) *Anal. Biochem.* **216,** 176–187
23. Borhan, B., Mebrahtu, T., Nazarian, S., Kurth, M. J., and Hammock, B. D. (1995) *Anal. Biochem.* **231,** 188–200
24. Gill, S. S., Ota, K., and Hammock, B. D. (1983) *Anal. Biochem.* **131,** 273–282
25. Morisseau, C., Goodrow, M., Dowdy, D., Zheng, J., Greene, J., Sanborn, J., and Hammock, B. (1999) *Proc. Natl. Acad. Sci. U. S. A.* **96,** 8849–8854
26. Argiriadi, M. A., Morisseau, C., Goodrow, M. H., Dowdy, D. L., Hammock, B. D., and Christianson, D. W. (2000) *J. Biol. Chem.* **275,** 15265–15270
27. Grant, D. F., Greene, J. F., Pinot, F., Borhan, B., Moghaddam, M. F., Hammock, B. D., McCutchen, B., Ohkawa, H., Luo, G., and Guenthner, T. M. (1996) *Biochem. Pharmacol.* **51,** 503–515
28. Laemmli, U. (1970) *Nature* **227,** 680–685
29. Mumby, S. M., and Hammock, B. D. (1979) *Anal. Biochem.* **92,** 16–21
30. Beetham, J. K., Tian, T., and Hammock, B. D. (1993) *Arch. Biochem. Biophys.* **305,** 197–201
31. Guex, N. (1996) *Experientia* (*Basel*) **52,** 26 (abstr.)
32. Guex, N., and Peitsch, M. C. (1996) *Protein Data Bank Quarterly Newsletter* **77,** 7
33. Guex, N. and Peitsch, M. C. (1997) *Electrophoresis* **18,** 2714–2723
34. Wixtrom, R. N., Silva, M. H., and Hammock, B. D. (1988) *Anal. Biochem.* **169,** 71–80
35. Rink, R., Spelberg, J. H. L., Pieters, R. J., Kingma, J., Nardini, M., Kellogg, R. M., Dijkstra, B. W., and Janssen, D. B. (1999) *J. Am. Chem. Soc.* **121,** 7417–7418
36. Blumenstein, J., Ukachukwu, V., Mohan, R., and Whaleen, D. (1993) *J. Org. Chem.* **58,** 924–932
37. Zou, J., Hallberg, B. M., Bergfors, T., Oesch, F., Arand, M., Mowbray, S. L., and Jones, T. A. (2000) *Struct. Fold. Des.* **8,** 111–122
38. Allen, F. H., and Kennard, O. (1993) *Chem. Design Automation News* **8,** 31–37
39. Ippolito, J. A., Alexander, R. S., and Christianson, D. W. (1990) *J. Mol. Biol.* **215,** 457–471
40. Ollis, D., Cheah, E., Cygler, M., Dijkstra, B., Frolow, F., Franken, S., Harel, M., Remington, S., Silman, I., Schrag, J., Sussman, J., Verschueren, K., and Goldman, A. (1992) *Protein Eng.* **5,** 197–211
41. Sussman, J., Harel, M., Frolow, F., Oefner, C., Goldman, A., Toker, L., and Silman, I. (1991) *Science* **253,** 872–879
42. Ordentlich, A., Barak, D., Kronman, C., Ariel, N., Segall, Y., Velan, B., and Shafferman, A. (1998) *J. Biol. Chem.* **273,** 19509–19517
43. Verschueren, K., Seljee, F., Rozeboom, H., Kalk, K., and Dijkstra, B. (1993) *Nature* **363,** 693–698
44. Bell, P. A., and Kasper, C. B. (1993) *J. Biol. Chem.* **268,** 14011–14017